Excess energies of *n*- and *i*-octane molecular clusters

Hanna Vehkamäki[a] and Ian J. Ford
Department of Physics and Astronomy, University College London, Gower Street, London WC1E 6BT, United Kingdom

(Received 22 May 2000; accepted 8 January 2001)

Cloud chamber data for the nucleation of droplets from supersaturated *n*- and *i*-octane vapors are analyzed using nucleation theorems. We obtain the excess energies of pure and mixed component molecular clusters with sizes ranging from 19 to 58 molecules. We plot this information in the form of an excess energy surface for a range of cluster compositions. Since the two species are similar we also combine the data into a plot of excess energy against the total number of molecules in the cluster. We show that the capillarity approximation fails to predict the critical cluster composition, though it does provide a rough estimate of the excess energy of a specified cluster. © *2001 American Institute of Physics.* [DOI: 10.1063/1.1351874]

I. INTRODUCTION

Doster *et al.*[1] have presented measurements of the rate of nucleation of droplets from pure *n*-octane and *i*-octane vapors, and from mixtures of the two species, obtained using a cloud chamber. The nucleation rates are determined as functions of the temperature T and the supersaturations, S_n and S_i, of the *n*- and *i*-octane vapors, respectively. S_n is defined as the ratio $p_n/p^s_{n,\mathrm{pure}}(T)$, where $p^s_{n,\mathrm{pure}}(T)$ is the saturated vapor pressure over pure liquid *n*-octane, and p_n is the partial pressure of *n*-octane vapor in the chamber. S_i is defined similarly. We have used the two-component nucleation theorems[2] to analyze the nucleation rate data, obtaining information about the excess energies of small one and two component molecular clusters of these species. We describe the nucleation theorems in Sec. II, the fit to the data in Sec. III, the extracted cluster properties in Sec. IV, and draw some conclusions in Sec. V.

II. NUCLEATION THEOREMS

The nucleation theorems are based on kinetic and thermodynamic models of the process of nucleation. We assume that the nucleation rate J can be expressed as $J=J_0\exp(-W^*/kT)$, where W^* is the work of formation of the critical cluster: the cluster which is equally likely to grow or decay under the prevailing conditions in the vapor. J_0 is the kinetic prefactor, which can be estimated,[2] and k is the Boltzmann constant. According to the (first) nucleation theorem[3–7] the number of molecules of *n*-octane, Δn_n^*, in the critical cluster is given by

$$\Delta n_n^* = \left(\frac{\partial \ln J}{\partial \ln S_n}\right)_{S_i,T} - \left(\frac{\partial \ln J_0}{\partial \ln S_n}\right)_{S_i,T}, \tag{1}$$

and a similar equation provides a relation between Δn_i^*, the number of molecules of *i*-octane in the critical cluster, and the partial derivative of $\ln J$ with respect to $\ln S_i$.

The second nucleation theorem[8–10,2] gives the excess energy of the critical cluster (the energy of the cluster minus the energies its constituent molecules would have in the pure bulk liquids at the same temperature and pressure) as

$$E_x^* = \left(\left(\frac{\partial \ln J}{\partial T}\right)_{S_n,S_i} - \left(\frac{\partial \ln J_0}{\partial T}\right)_{S_n,S_i}\right) kT^2. \tag{2}$$

Thus the dependence of J upon T gives the excess energy of a cluster whose molecular composition can be determined through the dependence of J upon the vapor supersaturations. Different experimental conditions correspond to critical clusters of various sizes, and so if sufficient data is available, properties of clusters of a variety of sizes and at different temperatures can be determined. This is the method which has been used previously to obtain plots of excess energy against size for a number of single component molecular clusters,[8–10] and more recently for a binary system.[2]

For single component systems, the dependence of the prefactor J_0 on temperature and supersaturation is known,[9] while for multicomponent vapors, estimates for the derivatives of the prefactor have to be made based on classical nucleation theory.[2] These estimates are believed to be reasonably robust, and the physico-chemical data needed to make them (and also to perform classical calculations of the cluster composition) are presented in the Appendix and by Doster *et al.*[1] Another matter is that the theorems given above are derived assuming the vapor is an ideal mixture of ideal gases: corrections to this approximation have been found to be unimportant and we so ignore them.[10]

III. FITTING THE DATA

In order to make use of Eqs. (1) and (2), we have to fit a function to the data to relate $\ln J$ to T, S_i, and S_n. Generalizing the fitting function used by Doster *et al.*[1] we chose to use the form

$$\ln J(T,S_\xi) = \ln(aT+b) + \frac{cT+d}{S_\xi} + eS_\xi + f \tag{3}$$

[a]Current address: Department of Physics, P.O. Box 9, 00014, University of Helsinki, Finland.

for pure *n*-octane and *i*-octane. The suffix ξ corresponds to *n* or *i*, and the coefficients *a*, *b*, *c*, *d*, *e*, and *f* are fitting parameters (different values for each pure case). This function produces a good fit not only to the pure vapor experimental data of Doster *et al.*,[1] but also to the pure *n*-octane data of Rudek *et al.*[11] Doster *et al.* have also measured nucleation rates for three mole fractions of *i*-octane in the vapor mixture: $X=1/2$, $X=1/4$, and $X=3/4$. Figures 4–6 of Doster *et al.*[1] suggest that for such mixtures of *n*-octane and *i*-octane the nucleation rate is a smooth function of the combined effective supersaturation $S^*=S_n^{(1-X)}S_i^X$. Guided by the apparent similarity of the plots of J as function of S^* in the mixed cases to the plots of J as a function of S_ξ in the pure cases we chose to fit the nucleation rate in the mixed cases using the form

$$\ln J(T,S_n,S_i)=\ln J(T,S^*)=\ln(aT+b)+\frac{cT+d}{S^*}+eS^*+f. \tag{4}$$

We fitted each of the mixed vapor datasets, with $X=1/2$, $X=1/4$, and $X=3/4$, separately. It must be noted that since S_n and S_i are combined into one variable, the above form with a fixed X leads to a firm relation between $(\partial \ln J/\partial \ln S_n)_{S_i,T}=(1-X)(\partial \ln J/\partial \ln S^*)_T\approx\Delta n_n^*$ and $(\partial \ln J/\partial \ln S_i)_{S_n,T}=X(\partial \ln J/\partial \ln S^*)_T\approx\Delta n_i^*$ and thus the mole fraction in the critical cluster $x^*=\Delta n_i^*/(\Delta n_i^*+\Delta n_n^*)\approx X$ is fixed for a certain X. This obviously restricts the generality of our analysis. In any case, the set of experimental points available leads to a restriction of this kind. The data points for each X happen to form lines in the three dimensional (T,S_n,S_i) space. We can actually find an equation for these lines, that is we can solve one of the variables as a function of two others; for example, $S_i=S_i(T,S_n)$. This means that from these data we are not able to derive independently the partial derivatives with respect to all three variables. Our approach is further supported by the fact that *i*-octane and *n*-octane molecules are very similar, and therefore it is likely that the mole fraction of the cluster closely reflects the mole fraction of the vapor.

Further support is given by the classical theory, based on the capillarity approximation, which predicts that $x^*\approx X$ holds accurately for the mixture of *n*-octane and *i*-octane. Note that in this paper x^* is the mole fraction of the entire nucleus including surface excess effects, not the mole fraction of the core of the cluster (for more details on the subject see Laaksonen *et al.*[12]).

We noticed that a subset of measurements with $X=1/4$ and $266.0\,\mathrm{K}<T<276.2\,\mathrm{K}$ showed a reduction in nucleation rate as the supersaturation of *i*-octane is increased, while the temperature and supersaturation of *n*-octane are kept constant. Including this subset within the fitting procedure caused the fit to behave unphysically, and thus we discarded this set, in the belief that it suffers from inaccuracies in the measurements.

Figures 1(a) and 1(b) show examples of the goodness of the fit. We studied the uncertainty of the fit (and hence the derived cluster properties) by using a modified fitting function where the coefficient *e* was multiplying $\ln S^*$ rather than S^*. Figure 1(b) also shows the classical nucleation rate curves for pure *i*-octane at five different temperatures. The curves are considerably shifted to the left, and the slopes differ as well.

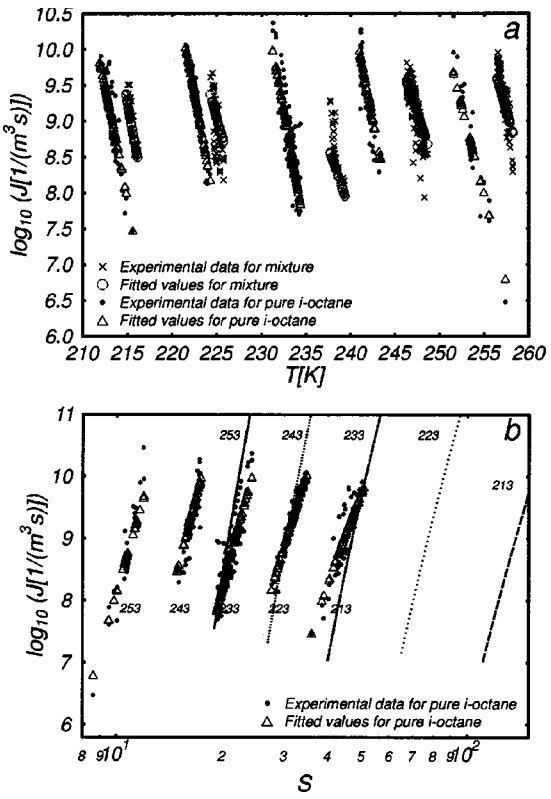

FIG. 1. Comparison between the actual measured values for the nucleation rate and the fitted values. Data points for pure *i*-octane are shown as a function of (a) temperature and (b) supersaturation *S*. Data for the mixture with $X=1/2$ are shown only against temperature. Other data were left out for graphical clarity. The lines in (b) represent classical nucleation rates for pure *i*-octane at five different temperatures. The upper numbers refer to the temperatures at which the classical curves were calculated, and the lower ones to the (only approximately constant) temperature of the pure *i*-octane data sets.

IV. CLUSTER PROPERTIES

Classical nucleation theory also yields predictions for the numbers of molecules in the critical cluster. Of course, they should not be trusted since the application of bulk material properties to small molecular clusters is hard to justify. The method for obtaining the classical values is explained elsewhere.[2,12] Figures 2 and 3 (for pure *i*-octane, and mixed clusters, respectively) compare the classical predictions for the *i*-octane molecular content of the critical clusters with those obtained from the experimental data.

The molecular numbers of *i*-octane in the critical cluster according to classical theory are shown on the horizontal axis, and are compared with other values on the vertical axis. First, the line representing classical data provides a one to one correspondence for reference purposes. The vertical bars show estimated error bars for the classical values. The method of obtaining the classical error estimates is explained in the Appendix. For mixed clusters (Fig. 3) we have also shown the number of *i*-octane molecules in the core of the cluster. The circles show the experimental values for the mo-

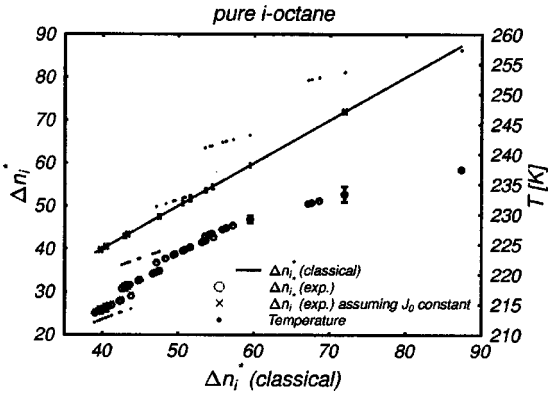

FIG. 2. The number of *i*-octane molecules in the critical cluster (under different experimental circumstances) for pure *i*-octane clusters. Predictions based on nucleation theorems and experimental data (circles) are shown in comparison with values obtained from the classical theory. The solid line shows the one-to-one correspondence representing classical theory. The crosses indicate the difference made by ignoring the contribution of the prefactor to the first nucleation theorem; they are practically indistinguishable from the circles. We have included the uncertainty in both the classical values and experimental points as vertical error bars attached to the solid line and the circles. For clarity, we have plotted only approximately every tenth point from the entire data set and show error bars only for selected points. We also show the temperatures corresponding to the experimental points.

lecular content of the critical cluster. We also show error bars to indicate uncertainties in the values extracted from the experimental data. For clarity, we have plotted only every tenth point, approximately, and have shown error bars only for selected points. The relative importance of the prefactor is indicated using cross symbols, by displaying the molecular content that would be extracted from the data by ignoring the S_i dependence of J_0. It is seen that the contribution arising from the prefactor is almost imperceptible for the pure clusters, but with mixed clusters the contribution increases slightly with the size of the cluster. The classical theory is quite unable to account for the critical sizes deduced from the data. The measurement temperature is also shown in Fig. 2. The temperature rises in the figure from left to right, so experiments as well as classical theory give smaller critical clusters at lower temperatures. In Fig. 3 the varying mole

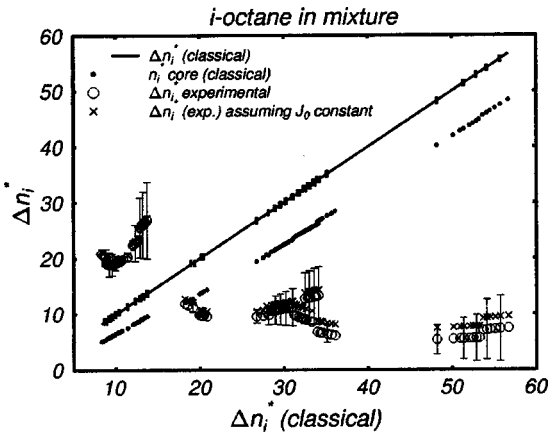

FIG. 3. As in Fig. 2, but for clusters containing both *i*-octane and *n*-octane. The dots show the number of *i*-octane molecules in the core of the cluster according to classical theory.

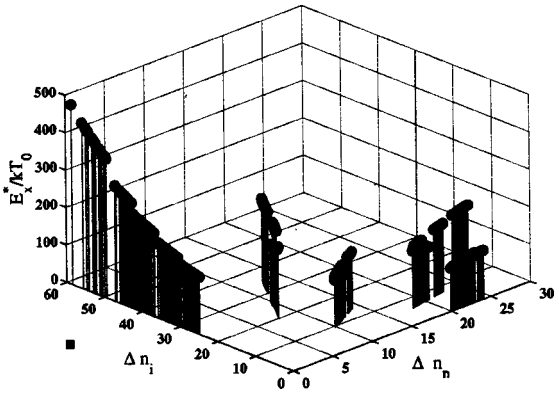

FIG. 4. The excess energy of the critical cluster as a function of the number of *i*-octane and *n*-octane molecules in the cluster. Note that the clusters are not all at the same temperature.

fraction blurs the picture, but when comparing cluster with equal compositions the same temperature dependence can be found. Even for this ideal system the surface excess numbers are found to be significant. The numbers of *n*-octane molecules in the critical clusters exhibit the same kind of behavior.

Figure 4 shows the excess energy of the critical cluster as a function of the number of *i*-octane and *n*-octane molecules in the cluster, as extracted from the experimental data. The energy is expressed in convenient units of kT_0, where $T_0 = 273.15\,\mathrm{K}$. The contributions of the prefactor to the excess energies in this plot lie between 28 kT_0 and 38 kT_0. The energy increases with the cluster size, and the points seem to lie on a reasonably smooth surface. Note, however, that the data correspond to clusters at a range of temperatures. For such clusters, the change in energy associated with a change in temperature of ΔT would be $C\Delta T$, where C is the heat capacity of the cluster. Estimating C to be of order $3k$ times the number of molecules in the cluster N, then the change in energy, divided by kT_0, would be of order $3N\Delta T/T_0$. For a cluster of 50 molecules this would make a contribution of about 30 to E_x/kT_0 for a dimensionless temperature range $\Delta T/T_0 = 0.2$, and it would therefore be necessary to correct for this effect in order to interpret the data fully.

Finally, we make use of the similarity in properties of *n*- and *i*-octane to display the cluster excess energies against the total number of molecules in the cluster in Fig. 5. There is reasonable consistency between the data for all the clusters. The excess energies obtained here from the experimental data of Doster *et al.*[1] are consistent with those extracted previously[9] from data gathered by Rudek *et al.*[13] Scatter is indicative of uncertainties in the fitting procedure, and experimental errors in the measurements. It should be kept in mind that the experimental points form separate, quasi-isothermal data sets which are separated by about 10 K. This causes uncertainties in the temperature derivatives of the nucleation rate and thus the excess energies. The error bars shown should be taken as lower limits of these uncertainties. However, the data are consistent with an underlying excess energy curve against cluster size. We have also included the classical predictions for the experimental points. The method

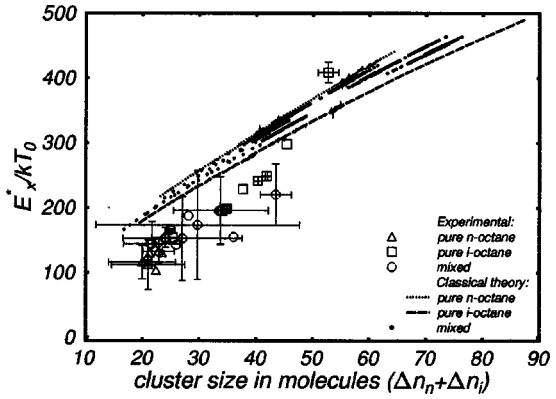

FIG. 5. The excess energy of the critical cluster as a function of the total number of *i*-octane and *n*-octane molecules in the critical cluster. The lines and dots show the classical predictions. The circles, squares, and triangles show the experimental values with error bars. For clarity, we have plotted only every tenth point (approximately) from the entire data set and have not included the error bars for all the points. The error bars for the classical values would be negligible in this picture.

for evaluating the classical energies was described previously.[2,12] The classical theory seems to predict the excess energy of a particular size quite well, although it fails to predict the critical size as indicated by Figs. 2 and 3. The latter is a consequence of different slopes of nucleation rate curves in Fig. 1(b). It must be noted that comparing the slopes of the classical curves shown in Fig. 1(b) with the slopes of the experimental data sets does not give an entirely true picture of the differences in the critical cluster sizes. We should compare the slopes at equal supersaturations and not at equal nucleation rates. For example, the classical nucleation rate for pure *i*-octane at $T=253\,\mathrm{K}$ and $S=10$ is $J \approx 10^{-8}/(\mathrm{m}^3\mathrm{s})$, and lies far below the bottom of the picture. Another factor is that the temperature is not strictly constant within the experimental datasets.

V. CONCLUSIONS

Nucleation theorems relate properties of the critical molecular cluster to the dependence of the nucleation rate on experimental control parameters such as the temperature and vapor supersaturations. Using theorems for two-component nucleation, we have analyzed droplet formation rate data for recent experiments involving pure *n*- and *i*-octane vapors, and mixtures of the two.

The largest mixed cluster studied contains 48 molecules, 35 of which are *i*-octane, and the smallest contains 19 molecules with only 10 *i*-octane molecules. We were also able to study pure *i*-octane clusters ranging in size from 24 to 58 molecules, and pure *n*-octane clusters from 19 to 24 molecules in size. There is an uncertainty of about 5 to 10 % in these numbers. Classical nucleation theory provides estimates which are quite at odds with these sizes. The key second nucleation theorem for multicomponent cluster formation[2] allows us to determine the excess energies of these clusters: the energies of the clusters minus the energies each constituent molecule would have in single component liquids at the same temperature and pressure. The excess energy will comprise, to a first approximation, a bulk mixing energy, and a surface energy due to unsatisfied bonds (undercoordination).

The excess energies of the clusters have been displayed in the form of an energy surface over cluster composition. We have gone on to convert the energy surface into a plot of excess energy against the total number of molecules in the critical cluster. This time, the classical theory is seen to give a reasonable estimate for the energy of cluster of a given size. However, due to the inability to predict critical sizes, the classical theory provides a poor model of nucleation rates, as shown by Doster *et al.*[1]

The data we have analyzed here, and elsewhere[8–10,2] provide a wealth of information about the small, short-lived molecular clusters that control the nucleation of droplets from metastable vapors. This information could be useful as reference material in numerical studies of the structure of these clusters.

ACKNOWLEDGMENT

The work was funded by the Academy of Finland under Project No. 64314.

APPENDIX: PHYSICO–CHEMICAL DATA

The properties of *i*-octane and *n*-octane liquids (densities $\rho_{i,n}$, surface tensions $\sigma_{i,n}$ and saturated vapor pressures $p^s_{i,\mathrm{pure}}$ and $p^s_{n,\mathrm{pure}}$) are given by Doster *et al.*[1]

The liquid phase is assumed to be ideal, and thus the activities $a_\xi(x_{\mathrm{bulk}},T)=p^s_\xi(x_{\mathrm{bulk}},T)/p^s_{\xi,\mathrm{pure}}(T)$, with $\xi=n,i$, take the simple forms $a_i(x_{\mathrm{bulk}},T)=x_{\mathrm{bulk}}$ and $a_n(x_{\mathrm{bulk}},T)=1-x_{\mathrm{bulk}}$. $p^s_\xi(x_{\mathrm{bulk}},T)$ is the saturated vapor pressure of component ξ over a flat surface of liquid mixture with *i*-octane bulk mole fraction x_{bulk}.

The molecular masses are $m_i=m_n=144.23\times 1.660\,57\times 10^{-27}\,\mathrm{kg}$. The latent heats of evaporation L_ξ for the pure liquids are evaluated using the Clausius–Clapeyron equation

$$\frac{dp^s_{\xi,\mathrm{pure}}}{dT}=\frac{L_\xi}{T(v^s_{v,\xi}-v^s_{l,\xi})}. \tag{A1}$$

If we assume that the molecular volume in the liquid $v^s_{l,\xi}$ is negligible compared with that in the saturated vapor $v^s_{v,\xi}$, we get $L_\xi(T)=kT^2/p_{\xi,\mathrm{pure}}\,dp^s_{\xi,\mathrm{pure}}/dT$.

To estimate the uncertainty of the classical predictions we have used slightly modified fits for the density and surface tension. Not only the absolute values but also the composition and temperature derivatives of these quantities have to be changed to perform a relevant sensitivity analysis. At most, the uncertainty in surface tension and density were taken to be 5%. As for the activities, we considered the mixture ideal even when performing the sensitivity analysis.

[1] G. Doster, J. Schmitt, and G. Bertrand, J. Chem. Phys. **113**, 7179 (2000).
[2] H. Vehkamäki and I. J. Ford, J. Chem. Phys. **113**, 3261 (2000).
[3] D. Kashchiev, J. Chem. Phys. **76**, 5098 (1982).
[4] Y. Viisanen, R. Strey, and H. Reiss, J. Chem. Phys. **99**, 4680 (1993).
[5] R. Strey and Y. Viisanen, J. Chem. Phys. **99**, 4693 (1993).
[6] D. W. Oxtoby and D. Kashchiev, J. Chem. Phys. **100**, 7665 (1994).
[7] Y. Viisanen, R. Strey, A. Laaksonen, and M. Kulmala, J. Chem. Phys. **100**, 6062 (1994).

[8] I. J. Ford, J. Chem. Phys. **105**, 8324 (1996).
[9] I. J. Ford, Phys. Rev. E **56**, 5615 (1997).
[10] M. Knott, H. Vehkamäki, and I. J. Ford, J. Chem. Phys. **112**, 5393 (1999).
[11] M. Rudek, J. Fisk, V. Chakarov, and J. Katz, J. Chem. Phys. **105**, 4707 (1996).
[12] A. Laaksonen, R. McGraw, and H. Vehkamäki, J. Chem. Phys. **111**, 2019 (1999).
[13] M. Rudek, J. Fisk, V. Chakarov, and J. Katz, J. Chem. Phys. **90**, 1856 (1989).